

STIX PFM Detector Performance Pre-Delivery Test Report STIX-TR-0108-FHNW

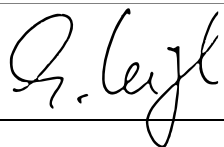


Issue: 1

Revision: 0

Date: 26 June 2017

Signatures & Approval

	Name	Signature	Date
Prepared by	Oliver Grimm		
Reviewed by	Säm Krucker PI		
Approved by	Francesca Molendini System Engineer		
Released by	Stefan Kögl Project Manager		

Change Log			
Issue / Rev.	Date	Author	Reason for Change
1 / 0	26 June 2017	O. Grimm	New document

Change Record			
Issue/Rev.	Description of Changes	Paragraph	Pages

Distribution List										
Name	Company	Issue / Revision								
STIX CDM										
ESA SO										

© Copyright: This document is intended for internal use. All rights to the documents and reports developed, both the written and machine-readable forms as well as the contents, are held by the FHNW.

Table of Content

1 SCOPE..... 4

1.1 APPLICABLE DOCUMENTS (AD)..... 4

1.2 REFERENCE DOCUMENTS (AD)..... 4

1.3 LIST OF ABBREVIATIONS..... 4

2 MEASUREMENT OVERVIEW..... 5

3 SPECTRAL RESOLUTION MEASUREMENTS 6

3.1 MEASUREMENT DETAILS 6

3.2 DATA PROCESSING..... 8

3.3 RAW AND CALIBRATED SPECTRA..... 8

3.4 RESULTS 11

3.4.1 Run 1 – Setting (A)..... 11

3.4.2 Run 4 – Setting (C)..... 12

3.4.3 Run 5 – Setting (B)..... 13

4 POWER-UP EFFECT ON HOUSEKEEPING VALUES 15

5 THRESHOLD SCAN..... 17

6 CONCLUSIONS..... 18

1 Scope

This document reports on the detector front-end performance measurements that were executed during the STIX thermal-vacuum test sequence.

It provides the data to show compliance of the STIX PFM as built model to the energy resolution and energy range requirements.

1.1 Applicable Documents (AD)

Ref. N	Doc. No.	Title Issue	Issue
[AD1]	SOL-EST-RCD-0050	Solar Orbiter Experiment Interface Document – Part A”	5.0
[AD2]	SO-STIX-EID-30001	Experiment Interface Document – B	6.0

Table 1-1: Applicable Documents

1.2 Reference Documents (AD)

Ref. N	Doc. No.	Title Issue	Issue
[RD01]	STIX-LI_0002_FHNW	STIX Abbreviations and Acronyms List	1.6
[RD02]	STIX-TN-0122-FHNW	STIX Essential Performance Test	1.0
[RD03]	STIX-PL-0101-FHNW	STIX PFM Environmental Test Plan and Specification	1.1
[RD04]	STIX-UM-0402-AOT	stac User and Reference Manual	1.0

Table 1-2: Reference Documents

1.3 List of abbreviations

The abbreviations are in accordance with the applicable documents, see [RD01]

2 Measurement overview

After completion of the thermal cycling program reported [RD02], STIX was left in stable thermal condition, with shroud and mounting plate temperature at +50°C and cold-element interface temperature at -25°C. This corresponds to the warmest operation condition in flight and thus the worst-case in term of detector energy resolution (as the semiconductor leakage current is highest).

The performance measurements followed the principles described in [RD02], as far as software functionality and schedule constraints allowed. In particular, test pulse scans and leakage current determination were not yet supported by the flight software and thus skipped.

3 Spectral resolution measurements

The spectral resolution measurement consisted in accumulating calibration spectra with the STIX internal barium-133 radioactive source with three different instrument settings:

(A) High voltage about -190 V, short shaping time (1.78 μ s, ASIC register set-point 1).

This corresponds to the nominal settings at the beginning of the mission. The short shaping time of the ASICs trades some energy resolution for higher counting rate.

The actual read-back is 198 V for the house keeping line HV_01_16_V and 193 V for HV_17_32_V.

(B) HV about -350 V, short shaping time

Semiconductors degraded by proton-induced displacement damage over the mission will need higher voltage to obtain their best energy resolution. The higher voltage reduces the tailing due to hole-carrier loss. Read-back 348 V / 327 V.

(C) HV about -190 V, long shaping time (4.95 μ s, ASIC register set-point 5)

The optimum energy resolution with non-degraded detectors is achieved in these conditions. Read-back as for (A).

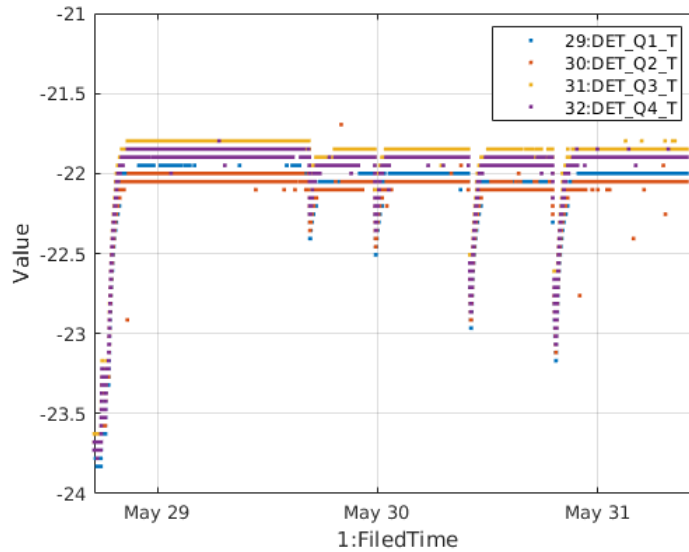
3.1 Measurement details

The performance measurements were done at the University of Bern, with data accumulated between 28 May 2017, 21:01, and 31 May 2017, 20:16 (see also the electronic log book at ihp-pc49.ethz.ch/STIXelog).

STIX was in MAINTENANCE mode. A calibration spectrum was accumulated every 40 minutes for all pixels and all detectors.¹ The house keeping system registered the following temperatures throughout the data accumulation: Detector circuit board -22°C, PSU +58 °C, Aspect System 50°C - 53°C, FPGA 62°C, IDPU circuit board 57°C.

The temperature stability over the measurement time can be seen on the following plot, giving the values of the four circuit boards temperature sensors. The attenuator temperature (ATT_T), the closest sensor registering the cold unit environment, registered a constant value of +47 °C.

¹ Every 40 minutes 128 TM(21,6)/SSID 41 packets, with spectral data for three pixels each arrived, with a cadence of three seconds (total duration about 6.5 minutes). Packets are send in detector order 1,2,3,...,30,31,0. For each detector, pixels are send in order 0,1,2,...,10,11.



A summary of the five measurement runs is given in the table below. To facilitate easier retrieval of the telemetry data in the future, the TM(21,6) source sequence count (SSC) is given as well, although it is not unique (restarts at zero after a reboot).

Run # (Setting)	Start time (UTC)	End time	SSC range
1 (A)	28 May 22:00	29 May 14:15	16 - 3215
2 (B)	29 May 17:10	29 May 23:13	3350 - 4629
3 (C)	30 May 00:21	30 May 09:01	4630 - 6421
4 (C)	30 May 10:44	30 May, 18:54	0 - 1663
5 (B)	30 May 19:59	31 May 7:31	0 - 2303

After Run 1 baseline, threshold, and test pulse scans were done, until about 16:40. The following two runs suffered from very low count rates, possibly due to an application software problem (which was not further investigated at the time). These runs are disregarded in the following, listed here only in case of later investigation. STIX was rebooted and the rate returned to normal. The remaining two run were thus always started with a reboot, consequently the SSC starts at counting at zero each time.

All ASICs were set to the same settings. The FPGA latency time was set to raw value 2 (3.9 μ s) for the short and to 5 (7.8 μ s) for the long shaping time. The trigger threshold of 62 corresponds approximately to an energy of 16 keV, as can be seen in the energy-calibrated spectra further below.

```

Register 1 (ICOMP)      0x1
Register 2 (IREQ)      0x4
Register 3 (TH)        all 62
Register 4 (SEL_TEST)  all off

```

Register 5 (TPEAK)	0x1 or 0x5
Register 6 (IO)	0x1
Register 7 (RDELAY)	0x0
Register 8 (GAIN)	0x3
Register 9 (SPY)	0x0
Register 10 (VREF2P)	0x3
Register 11 (TUNE)	0x2 (baseline holder off)
Register 12 (ALIMON)	all on

3.2 Data processing

All telemetry obtained from STIX over SpaceWire is registered and archived by the SIIS. For post-processing, the required telemetry packets are extracted with the SIIS Archive Browser. For the performance measurements reported here, a further program (TMConvert, see below), is used to translate the spectral data contained in TM(21,6)/SSID 41 into the same format that is employed by the `stac` program (STIX-UM-0402, I1R0, see page 7 for the format), used during STIX development for detector and front-end studies. Therefore, the same Matlab-based analysis tools could be used.

TMConvert is a C++ program that reads a telemetry file exported with the SIIS Archive Browser in ASCII format and performs conversion for a number of telemetry services, typically producing some console and/or text file output.² It is also used to process housekeeping TM(3,25) data. For TM(21,6)/SSID 41, the console output looks like the following:

```
Packet 2331  PID 93, category 12, length 3153, grouping 0, SSC 132
              Type 21, subtype 6, coarse time 2147496823, fine time 40042
              SIIS time stamp 1496009391.807 - UTC Sun May 28 22:09:51 2017

SSID 41: Duration 2000, quiet time 0, live time 390945, average temperature 0
Detector mask ffffffff (N=32), pixel mask fff (12), subspectrum mask 1 (1)
Subspectrum 0: Points 1024, summed channels 1, lowest channel 0

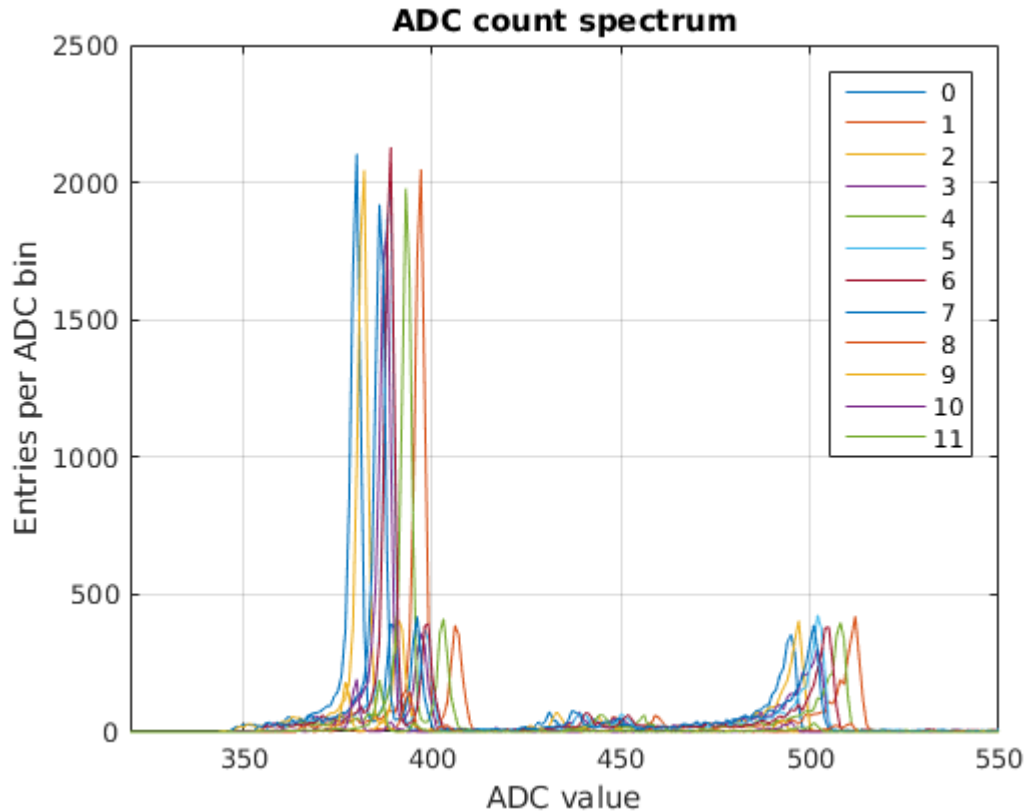
--- Number of structures: 3 ---

Structure 0:   Detector 30, pixel 0, subspectrum 0, number of points 1024
Structure 1:   Detector 30, pixel 1, subspectrum 0, number of points 1024
Structure 2:   Detector 30, pixel 2, subspectrum 0, number of points 1024
```

3.3 Raw and calibrated spectra

The raw data that are extracted from the telemetry result in an ADC spectrum, as shown in the following example which is taken from Run 1, showing the 12 pixels of detector 5.

² The program is available in the STIX subversion repository, currently at <https://projecthost.cs.technik.fhnw.ch/i4ds/stix/svn/Software/TMConvert>. The Matlab analysis tools and `stac` are also checked into this repository.

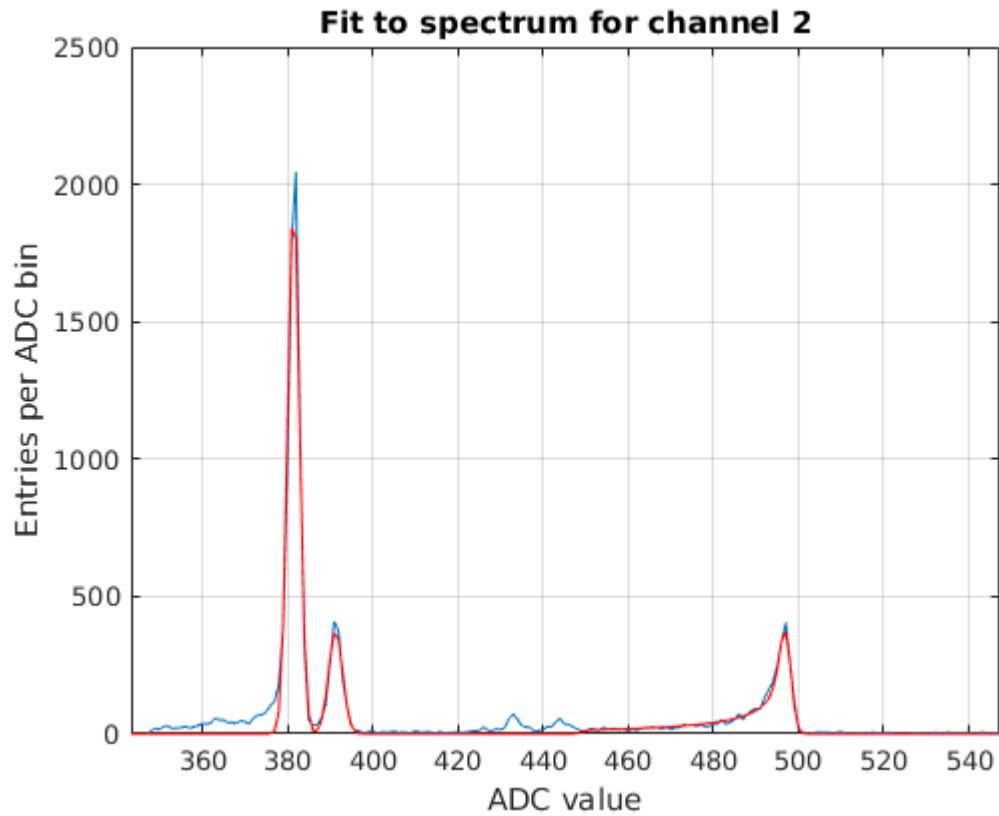


Due to the expected different amplification characteristics of each ASIC channel, the spectra are displaced with respect to each other.

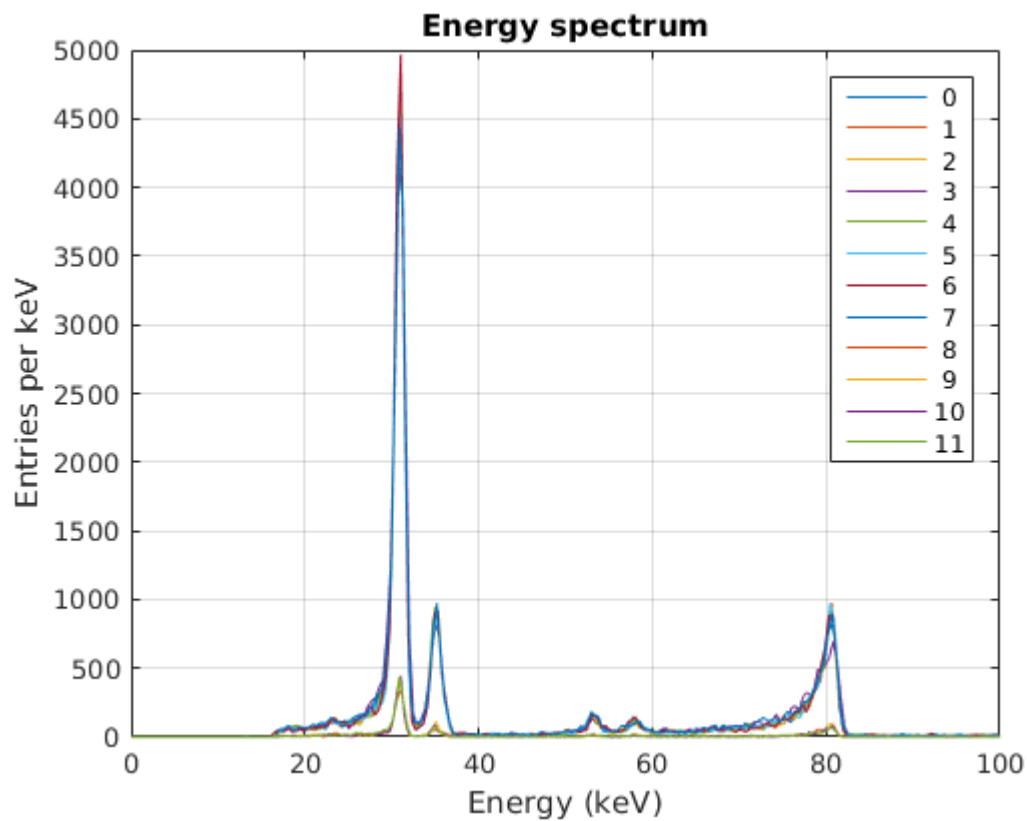
Pixel-by-pixel the spectra are then energy calibrated³. The fit to the 31 keV, 35 keV, and 81 keV lines of the radioactive source for the large pixel L2 looks like the following picture.

The procedure results in the best-fit ADC channels that correspond to the main lines at 31 keV and 81 keV. From this, the offset and gain for each channel is determined. The full-width-half maximum (FWHM) at these two energies is also extracted from the calibrated spectrum.

³ The principle is documented in the paper *Performance and qualification of CdTe pixel detectors for the Spectrometer/Telescope for Imaging X-rays*, 2015 JINST 10 C02011, doi:10.1088/1748-0221/10/02/C02011.



Finally, the resulting energy-calibrated spectrum in this case is the following.



The summary of the fit for all channels of detector 5 is as follows:

Channel	Location of Gain				Offset	FWHM (keV)		Histogram entries	
Pixel	31 / 81 keV (eV/count)				(counts)	31 / 81 keV		31+35 / 81 keV	
0	L0	380	495	431.7 ± 0.31%	308 ± 0.3	1.41	1.78	8258	3100
1	L1	397	513	431.6 ± 0.29%	325 ± 0.3	1.41	1.80	8258	3212
2	L2	381	498	431.0 ± 0.27%	310 ± 0.3	1.40	1.71	8261	3154
3	L3	387	502	435.5 ± 0.42%	316 ± 0.4	1.62	2.51	8310	3636
4	L4	393	509	432.5 ± 0.31%	322 ± 0.3	1.39	1.72	7887	3189
5	L5	388	503	436.7 ± 0.27%	318 ± 0.3	1.33	1.70	7816	3309
6	L6	389	505	428.5 ± 0.29%	317 ± 0.3	1.33	1.80	8131	3261
7	L7	386	501	432.9 ± 0.32%	315 ± 0.4	1.47	2.06	8064	3576
8	S8	393	511	425.5 ± 0.40%	321 ± 0.4	1.29	1.22	537	203
9	S9	377	493	430.7 ± 0.31%	305 ± 0.3	1.04	1.25	580	244
10	S10	380	495	432.0 ± 0.45%	308 ± 0.4	1.10	1.42	566	217
11	S11	386	502	431.7 ± 0.41%	314 ± 0.4	1.26	1.41	571	227

3.4 Results

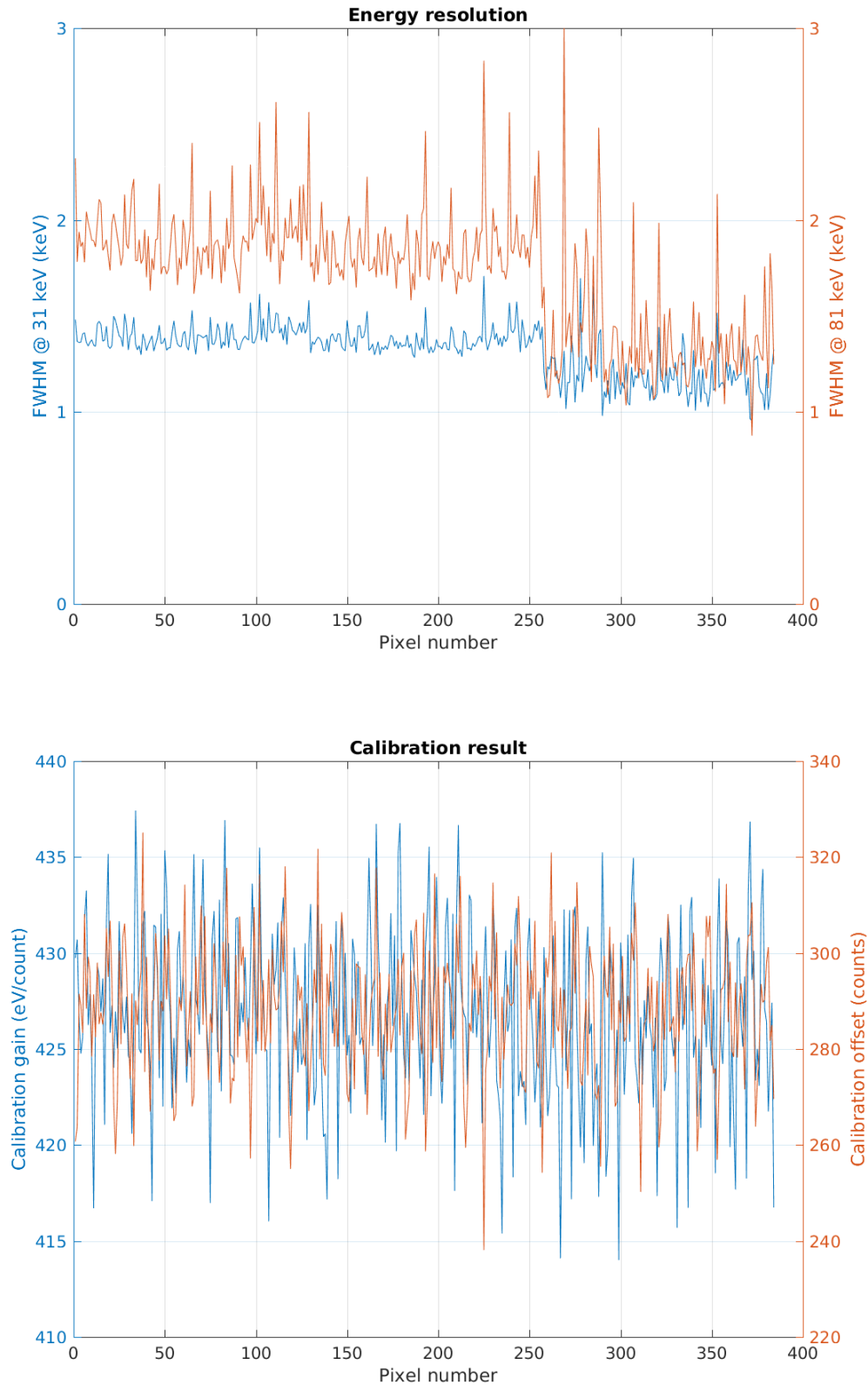
The main performance characteristic of the front-end is the energy resolution. This is shown in the following plots for all $32 \times 12 = 384$ pixels. The blue curve shows the FWHM at 31 keV, the red one at 81 keV. Due to the nature of the asymmetric higher energy line, the fitting works less precise, and thus the fluctuations are larger.

The small pixels can be identified by their systematically better energy resolution.

3.4.1 Run 1 – Setting (A)

The total number of counts accumulated during this run is 4'335'940 (count rate 74 s^{-1}). The number of counts per detector is in the range 125000 to 160000.

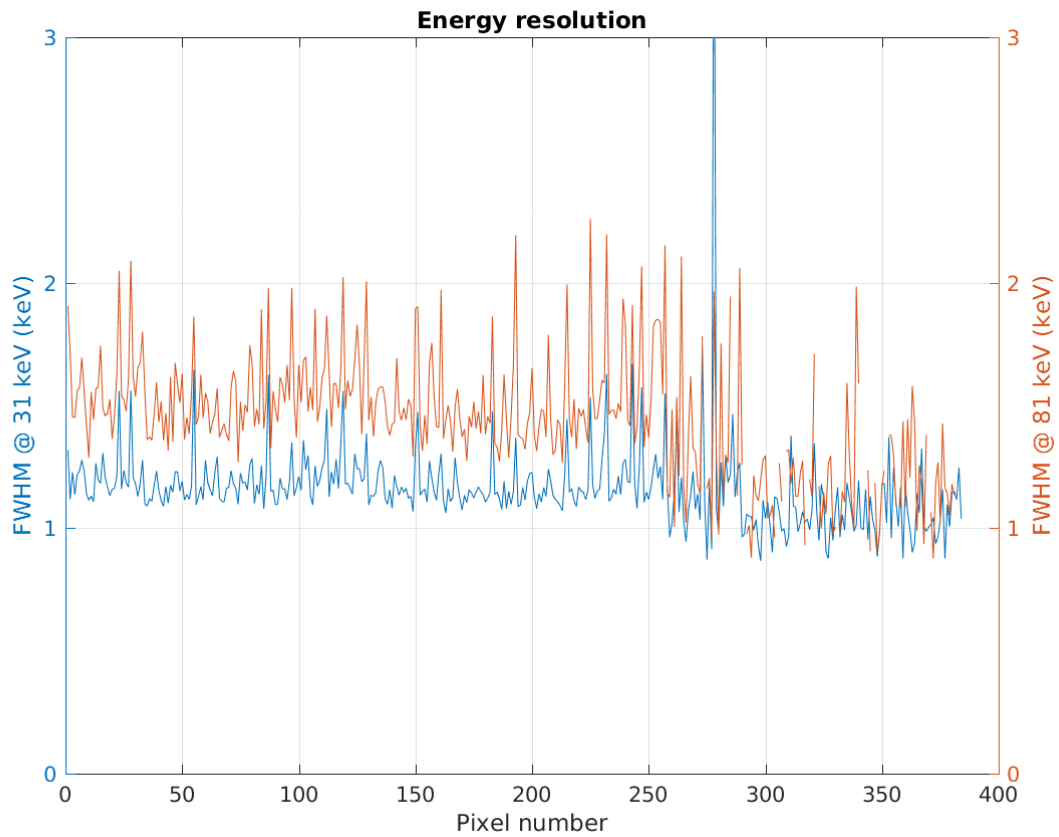
Exemplary for this run, the results for offset and gain are also shown for all pixels. There is only a small spread, indicating the good functioning of all detectors and all pixels. This is the case also for the other two runs for which the data is not shown.



3.4.2 Run 4 – Setting (C)

This run confirms that 1 keV FWHM energy resolution is systematically achievable for the small pixels with the longer shaping time.

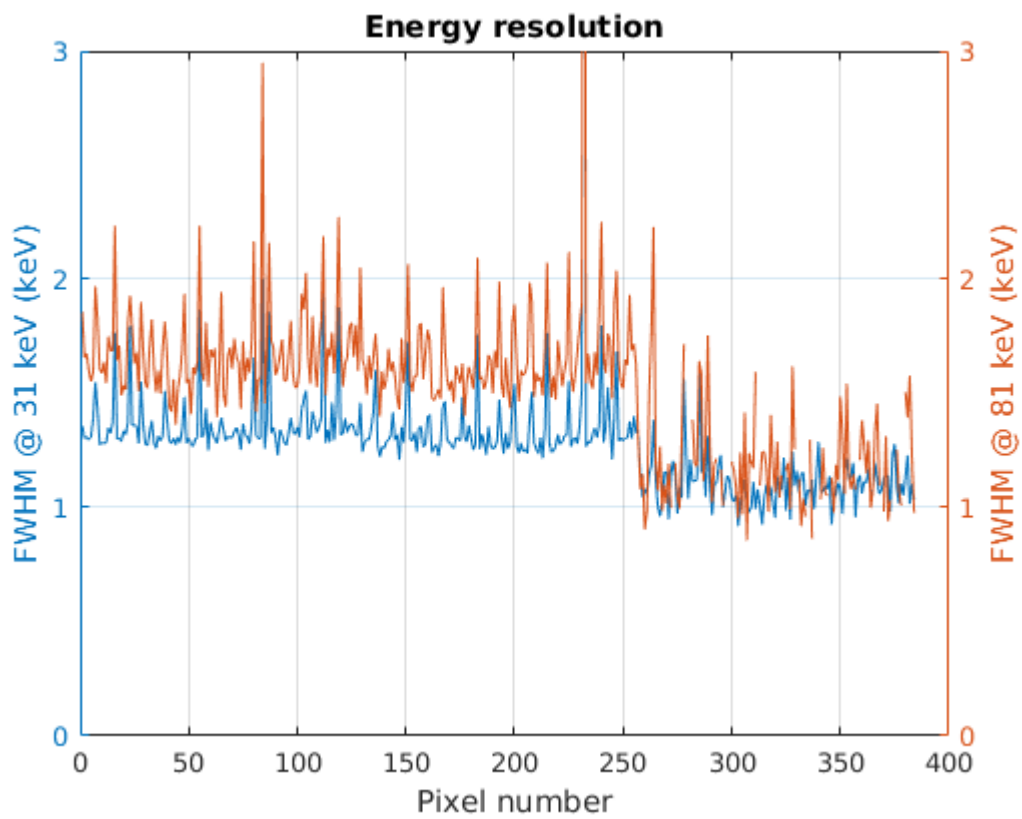
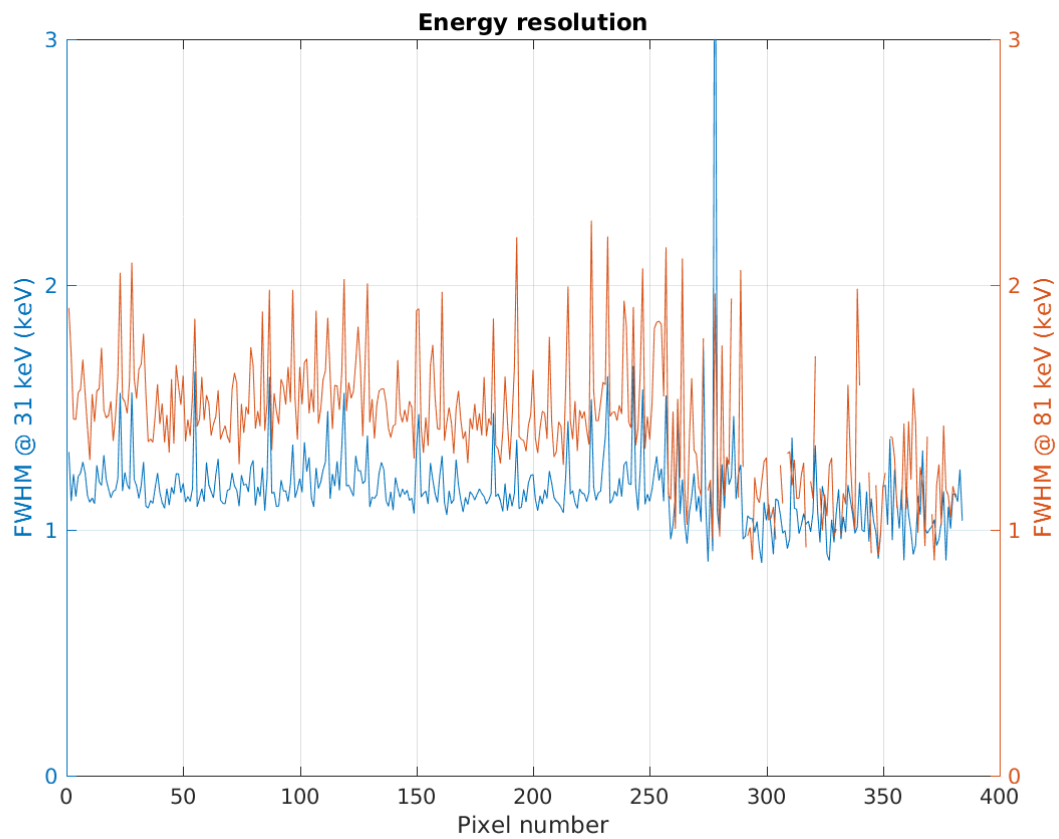
The total number of counts is 2'561'814 (count rate 87 s^{-1})..



3.4.3 Run 5 – Setting (B)

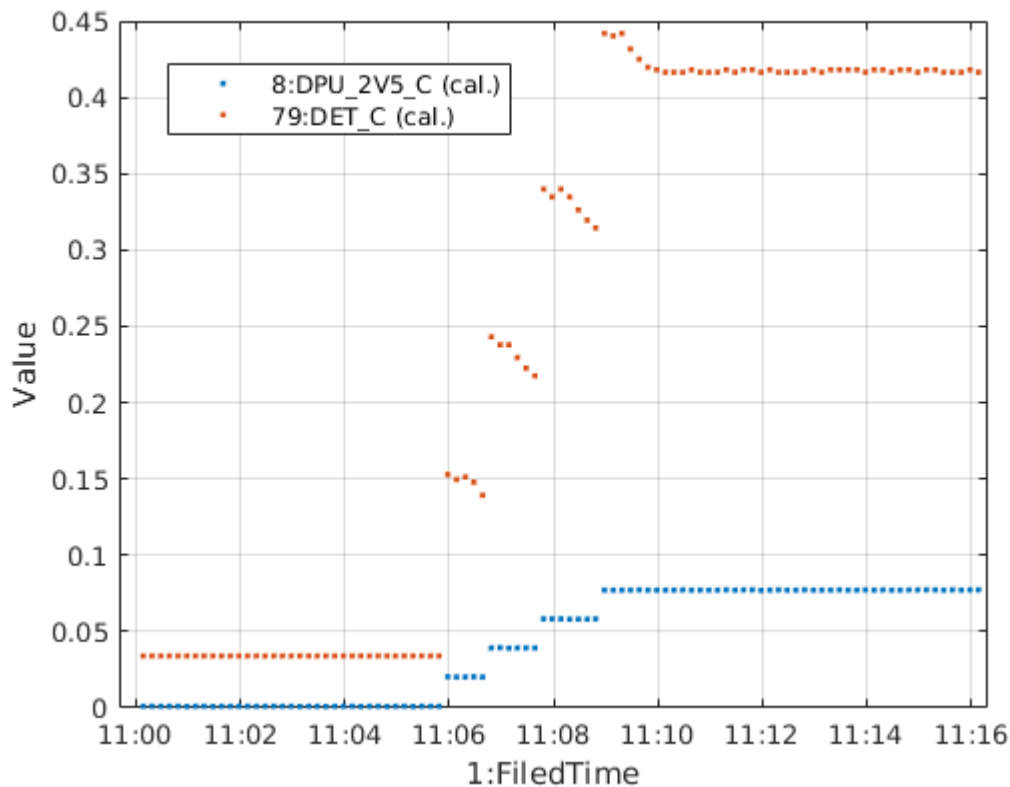
With the higher bias voltage, the hole-tailing is reduced for the higher-energy line, resulting in more symmetric lines and somewhat better FWHM. However, the overall leakage current is increased, and the energy resolution becomes more dependent on the exact pixel characteristics, seen in the more spiky appearance of the plot.

The total number of counts is 2'705'463 (count rate 65 s^{-1}).



4 Power-up effect on housekeeping values

The two housekeeping (HK) values that are mainly affected by the front-end power-up are the currents DPU_2V5_C and DET_C. The following plot shows their currents during step-wise switch-on of the four front-end quarters.⁴



This measurements has been not been performed during the TVAC testing, but at PSI in ambient environmental conditions.⁵

The current increase corresponds to about $2.5 \text{ V} \times 77 \text{ mA} / 4 = 48 \text{ mW}$ extra power per quarter on the 2.5 V IDPU line, and to $4.6 \text{ V} \times 390 \text{ mA} / 4 = 450 \text{ mW}$ for DET_C. The majority of the detector power is consumed on the warm back-end in the voltage regulators that generate the 3.3 V front-end supply and support electronics.

The decrease of DET_C after each switching step is due to the charging of the front-end filter capacitors.

⁴ The current values are determined using the nominal ADC-to-physical housekeeping calibration constants.

⁵ The switch-on sequence was too fast during TVAC testing, so the step-wise changes were not clearly registers in the TM(3,25)/SID 2 housekeeping packets that occur with 10 seconds cadence. The plotted data were taken on 26 June 2017 between 11:00 and 11:20. The current for all quarters powered up is identical in both cases for DPU_2V5_C, and about 10% higher at PSI for DET_C.

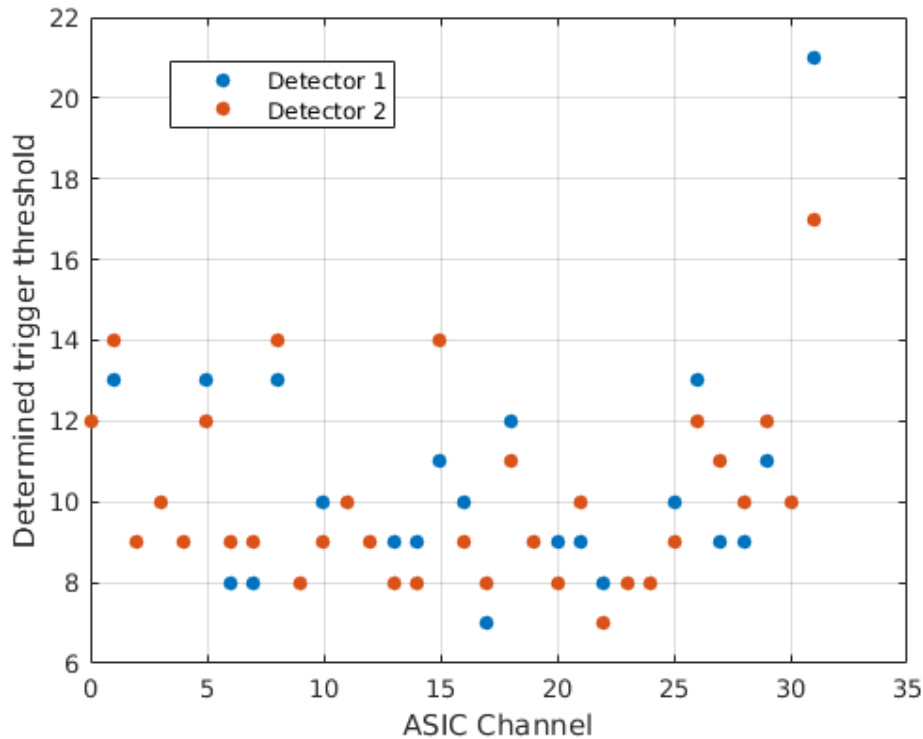
The SIIS current on the 28 V line increases by about 30 mA (corresponding to 840 mW) for each quarter. The majority of this is consumed in the IDPU, as the above plot shows.

Switching on the detector front-end has also some small effects on other HK values. These are reported here for reference. Note that most of the effects are very small, typically not much larger than the measurement scatter.

- DPU_2V9_V drops by 6 mV
- DPU_SPW0/1_V increases by 3.5 mV
- DPU_SPW_C drops by 10 ADC counts
- DPU_3V3_C changes from a narrow band of 994 ± 4 ADC counts to a wide band with values between 1000 and 1200 counts
- DPU_1V5_C changes from 716 ± 4 ADC counts to 716 ± 20 counts

5 Threshold scan

The threshold scan resulted in non-zero data for only two out of all 32 detectors (likely due to a software limitation).⁶ The obtained thresholds for zero bias voltage are shown in the following plot. Note that if there is only one orange dot shown for a channel, the blue dot is at the same value.



The threshold scan works by raising, channel by channel, the trigger threshold of each ASIC channel from zero until less than a given number of triggers are detected in a given time (see [RD04]). Here, the time is set to 1 second, and the limiting number of triggers to 10. For reference, a threshold of 10 corresponds to a photon energy of approximately 1.4 keV, and a threshold of 14 to 2.2 keV.

Large pixels are connected to channels 0, 1, 5, 8, 15, 18, 26, 29, as can be seen by the slightly higher trigger threshold (due to higher capacity, and thus higher electronic noise, of the larger area pixels). Small pixels are on channels 3, 11, 21, 30, and the guard ring to channel 31. All other channels are not connected.

This confirms that the electronic noise is very low for all 12 pixels, and that trigger thresholds well below 4 keV are achievable.

⁶ The scan is started with the telecommands (see electronic logbook, 29 May 2017, 15:12)
ZIX39011 {PIX00248 0xFFFF} {PIX00053 0xFFFFFFFF} {PIX00049 10} {PIX00055 1} and
ZIX39011 {PIX00248 0xFFFF0000} {PIX00053 0xFFFFFFFF} {PIX00049 10} {PIX00055 1}.
The ASIC shaping time and FPGA latency set-points are 1. The commands result in a TM(239,12)
after about 12 minutes. The SSC for the two received packets are 11 and 12.

6 Conclusions

The resolution measurements reported in Section 3 indicate that at 31 keV photon energy an energy resolution of 1 keV FWHM is achievable for the small pixels with a shaping time of 5 μ s, and 1.2 keV FWHM for the large pixels.

Previously reported data⁷ indicate that the cadmium K α escape line at 7.9 keV has a FWHM of 1 keV when the line at 31 keV had a width of 1.2 keV, so **the STIX energy resolution requirement of 1 keV at 5 keV photon energy is expected to be met.**

Investigations into the lowest possible trigger threshold have not been carried out due to schedule constraints. The threshold of the present measurements was set to 16 keV by the ASIC setting. The data mentioned above indicate for similar values of the energy resolution a trigger threshold at 3 keV. This is confirmed by the results in Section 5 that show a sufficiently low electronic by means of the minimum trigger threshold.

The highest energies measureable with the given ASIC settings can be calculated from the calibration constants reported in Section 3.3 and the maximum ADC count of 1023. This results in a value near to 300 keV. Note, however, that the non-linearity of the ASIC analogue output becomes noticeable above about 150 keV.

These measurements conclusively demonstrate that all 32 detectors of the STIX front-end work as expected, with no detectable performance degradation due to handling, assembly, or due to the analogue, digital or power supply electronics.

⁷ See Figure 5 in: The Spectrometer Telescope for Imaging X-Rays on board the ESA Solar Orbiter spacecraft, Nuclear Instruments and Methods in Physics Research A732, 295–298 (2013), doi:10.1016/j.nima.2013.05.050